

Magnetic flux penetration into $(\text{Tl}_{0.6}\text{Pb}_{0.5})(\text{Ba}_{0.1}\text{Sr}_{0.9})_2\text{Ca}_2\text{Cu}_3\text{O}_x$ and $(\text{Tl}_{0.8}\text{Bi}_{0.3})(\text{Ba}_{0.1}\text{Sr}_{0.9})_2\text{Ca}_2\text{Cu}_3\text{O}_y$ bulk pellet samples

A. Cigáň¹, B. Andrzejewski², G. Plesch³, G. Gritzner⁴, J. Maňka¹, V. Zrubec¹

¹ Institute of Measurement Science, Slovak Academy of Sciences, Dúbravská cesta 9, 842 19 Bratislava, Slovakia

² Institute of Molecular Physics, Polish Academy of Sciences, Smoluchowskiego 17, 60-179 Poznań, Poland

³ Department of Inorganic Chemistry, Faculty of Natural Sciences, Comenius University, 842 15 Bratislava, Slovakia

⁴ Institut für Chemische Technologie Anorganischer Stoffe, Johannes Kepler Universität, A-4040 Linz, Austria

Abstract

Magnetic field penetration into $(\text{Tl}_{0.6}\text{Pb}_{0.5})(\text{Ba}_{0.1}\text{Sr}_{0.9})_2\text{Ca}_2\text{Cu}_3\text{O}_x$ and $(\text{Tl}_{0.8}\text{Bi}_{0.3})(\text{Ba}_{0.1}\text{Sr}_{0.9})_2\text{Ca}_2\text{Cu}_3\text{O}_y$ bulk pellet samples was investigated by two methods: (i) by the volume magnetization and (ii) by the local scanning Hall method. Pb-doping resulted in stronger inter-grain links and improved the intra-grain critical current densities. Bi-doping instead of Pb-doping increased the critical temperature from 113 K to 116 K. Considering that bulk pinning of the doped Tl-1223 samples is low and that the magnetic field penetration is predominantly determined by geometrical barrier effects, the characteristic magnetic penetration fields obtained by the two methods are in excellent agreement.

1. Introduction

The knowledge of the magnetic penetration properties into the high- T_c superconducting materials provides useful information about the critical magnetic fields which are fundamental mixed-state parameters of the superconductors of type II. Several methods to study the magnetic field penetration into superconductors such as magneto-optic techniques, surface scanning of local magnetic fields by Hall probe, SQUID or others magnetic sensors are available. A classical method to determine the characteristic magnetic fields in type II superconductors is the measurement of the magnetization as a function of the applied magnetic field. Usually the volume (nonlocal) characteristics are measured. For example, the first deviation from the initial linear behavior of the magnetization versus the field may be attributed to the lower critical field H_{c1} . For high- T_c superconductors, the situation is far more complex due to their layered structure, to granularity, flux pinning and barrier effects. A rigorous treatment of this very complex problem is out of the scope of this paper. Our intention is to present the first penetration magnetic field characteristics obtained by two different methods, namely by volume magnetization and by local scanning Hall methods on Tl-1223 samples doped with Pb ((Tl,Pb)-1223) or Bi ((Tl,Bi)-1223) and to compare their superconducting and penetration properties.

2. Experimental

The bulk superconducting materials were prepared following a method described in [1] via a two step process. In the first step an aqueous solution of strontium, barium, calcium and copper nitrates (molar ratio 1.8 : 0.2 : 2 : 3) was evaporated to dryness and the residue was calcined at 900 °C for 30 h. Appropriate amounts of Tl_2O_3 , PbO or Bi_2O_3 were then added by co-milling to obtain powders with the starting composition of $(\text{Tl}_{0.6}\text{Pb}_{0.5})(\text{Ba}_{0.1}\text{Sr}_{0.9})_2\text{Ca}_2\text{Cu}_3\text{O}_x$ and of $(\text{Tl}_{0.8}\text{Bi}_{0.3})(\text{Ba}_{0.1}\text{Sr}_{0.9})_2\text{Ca}_2\text{Cu}_3\text{O}_y$. The above mixtures were uni-axially compacted at 1 GPa, wrapped in a silver foil and sintered in flowing oxygen at 925 °C for 12 min and at 910 °C for 10 h.

The experimental equipment for X-ray diffraction as well as for measuring the critical temperatures by the four – point technique has been described elsewhere [1].

The AC and DC virgin volume magnetization characteristics were measured by means of a

second order SQUID gradiometer, employing the compensation method after zero-field cooling at 77 K in magnetic fields ranging from 10^{-1} to 10^5 A m $^{-1}$ [2]. For AC magnetization measurements a frequency of 0.1 Hz was used. An applied magnetic field H_a was gradually increased in steps of 20, 40, 60, 80 and 100 % of the maximum amplitude in each significant range. For both AC and DC magnetization the applied magnetic field was parallel to the axis of the sample. The demagnetizing factor was determined from the dimensions of the pellet sample [3]. The first penetration magnetic field H_{p1}^{wl} of the inter-grain weak link network was obtained from the first deviation from linearity of the virgin DC magnetization curves.

A laboratory-made field imaging device was used to investigate the flux distribution inside the samples. The flux distribution was imaged by means of a cryogenic, axial Hall-probe. The probe had an active area of 0.2×0.2 mm and an accuracy of 8 A/m. The Hall-probe was driven by an X-Y positioning stage controlled by a PC computer. The X-Y position accuracy was equal to 0.1×0.1 mm. The samples and the probe were immersed directly into liquid nitrogen. All the measurements were performed at 77 K. The field generated by Helmholtz coils fixed outside the liquid nitrogen container was parallel to the axis of the sample. The experiments were performed in fields ranging from 0 to 7960 A/m. The laboratory residual field equal to about 40 A/m was not compensated.

3. Results and discussion

According to the X-ray diffraction data the samples consisted of almost phase-pure polycrystalline Tl-1223 phase. Very small amounts of Tl-1212 were present in both samples.

For $(\text{Tl}_{0.6}\text{Pb}_{0.5})(\text{Ba}_{0.1}\text{Sr}_{0.9})_2\text{Ca}_2\text{Cu}_3\text{O}_x$ a $T_{c(0)}$ value of 113 K was obtained. The $T_{c(0)}$ value for $(\text{Tl}_{0.8}\text{Bi}_{0.3})(\text{Ba}_{0.1}\text{Sr}_{0.9})_2\text{Ca}_2\text{Cu}_3\text{O}_y$ was 116 K. In both cases transition widths of 2.5 K were observed.

AC magnetization M versus the applied field H_a for the Tl-1223 samples with nominal compositions of $(\text{Tl}_{0.6}\text{Pb}_{0.5})(\text{Ba}_{0.1}\text{Sr}_{0.9})_2\text{Ca}_2\text{Cu}_3\text{O}_x$ and $(\text{Tl}_{0.8}\text{Bi}_{0.3})(\text{Ba}_{0.1}\text{Sr}_{0.9})_2\text{Ca}_2\text{Cu}_3\text{O}_y$ for different amplitudes of the magnetization field H_a are shown in Figs. 1 and 2. Fig. 1 shows M vs H_a hysteresis loops of the samples at magnetization fields sufficient for the penetration into the inter-grain and also intra-grain region.

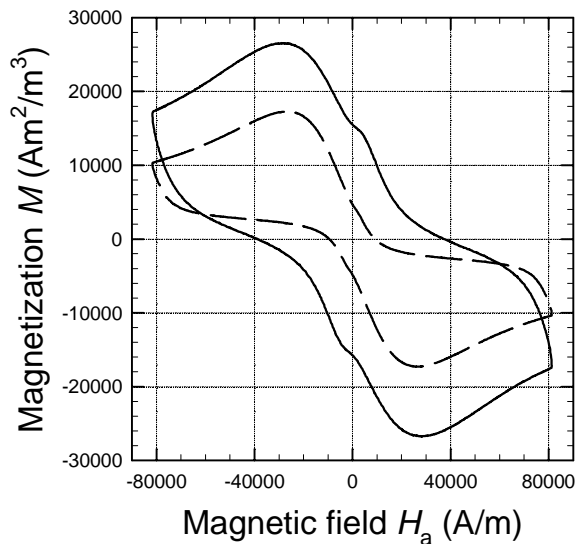


Figure 1. AC magnetization M versus the applied field H_a for Tl-1223 samples of nominal compositions of $(\text{Tl}_{0.6}\text{Pb}_{0.5})(\text{Ba}_{0.1}\text{Sr}_{0.9})_2\text{Ca}_2\text{Cu}_3\text{O}_x$ and of $(\text{Tl}_{0.8}\text{Bi}_{0.3})(\text{Ba}_{0.1}\text{Sr}_{0.9})_2\text{Ca}_2\text{Cu}_3\text{O}_y$ at given amplitude of the magnetizing field. (Tl, Bi)-sample: dashed line).

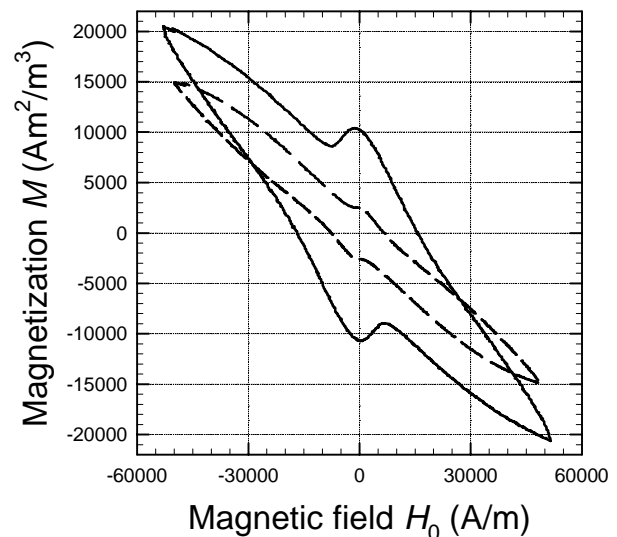


Figure 2. AC magnetization M versus the applied field H_0 (corrected by the demagnetization factor) for Tl-1223 samples of nominal compositions of $(\text{Tl}_{0.6}\text{Pb}_{0.5})(\text{Ba}_{0.1}\text{Sr}_{0.9})_2\text{Ca}_2\text{Cu}_3\text{O}_x$ and of $(\text{Tl}_{0.8}\text{Bi}_{0.3})(\text{Ba}_{0.1}\text{Sr}_{0.9})_2\text{Ca}_2\text{Cu}_3\text{O}_y$ at given (lower) amplitude of magnetizing field. (Tl, Bi)-sample: dashed line.

The greater hysteresis and magnetization of the Tl-1223 sample doped with Pb indicate higher intra-grain critical current densities. A comparison of the hysteresis loops of the two Tl-1223 samples at lower amplitude of H_a is given in Fig. 2. The more marked hysteresis and bump in the M vs H_a curve of the (Tl,Pb)-1223 sample point to a more than twofold inter-grain critical current density. The inter-grain junctions of the (Tl,Pb)-sample are more strongly connected than those in the (Tl,Bi)-1223 sample. Based on the results of scanning M vs H_a dependency for different values of magnetization field amplitude (not shown in this paper), better field dependence of critical current density or the existence of inter-grain cluster loops with higher currents for to (Tl,Pb)-sample can be inferred. From the DC magnetization M vs H_a dependency the first characteristic penetration magnetic fields after demagnetizing correction $H_{p1}^{wl} \sim 13.3$ and 8.6 A m^{-1} for the (Tl,Pb)- and the (Tl,Bi)-sample, respectively, were estimated.

The typical flux distribution obtained by Hall probe scanning for the (Tl,Pb)-sample in ZFCS procedure (the sample was first zero field cooled, then the screening of the applied DC magnetic field H was imaged) in a field equal to 796 A/m is shown in Fig. 3. The perfect symmetry of flux distribution, which proves the good homogeneity of the sample, was preserved in all fields. A similar symmetric distribution of the magnetic flux and a very good homogeneity of the specimen was found also for the (Tl,Bi)-sample. Due to the circular symmetry it is sufficient to perform one scan along sample diameter instead of the full flux distribution map.

The screening of the magnetic field by a superconductor can be described by the “screening function” F introduced by Reich et al. [4]. F for homogeneous field is defined as:

$$F(d, h_p, R, H) = \frac{H_z}{H}$$

where: h_p is the distance between the probe and the surface of the sample, H is the applied DC field and H_z is the value of the field above the surface of the superconductor. In the case when the magnetic field is not shielded by the sample the value of H_z approaches the value of H or function $(1-F)$ approaches the zero. Fig. 4 presents the dependence of $(1-F)$ on the applied field for the (Tl,Pb)- and the (Tl,Bi)-samples. In the low field region below 400 A/m , the magnetic flux mainly penetrates the sharp edges of the samples which causes a rapid decrease of the screening properties and of the $(1-F)$ value. The plateau shown in Fig. 4 in fields from 400 - 1100 A/m , may be explained using the Bean critical state model.

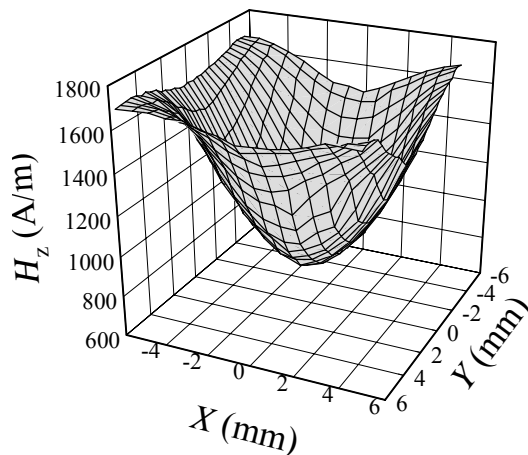


Figure 3. Field distribution over the $(\text{Tl}_{0.6}\text{Pb}_{0.5})(\text{Ba}_{0.1}\text{Sr}_{0.9})_2\text{Ca}_2\text{Cu}_3\text{O}_x$ -sample imaged in ZFCS procedure at the applied field $H = 796 \text{ A/m}$.

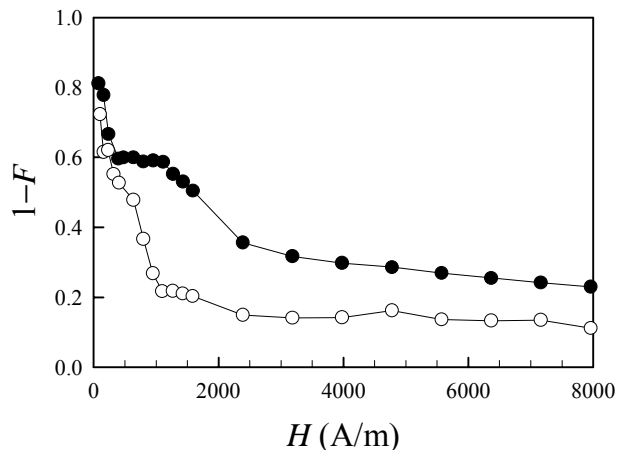


Figure 4. Dependencies of the $1-F$ function on the applied magnetic field H for $(\text{Tl}_{0.6}\text{Pb}_{0.5})(\text{Ba}_{0.1}\text{Sr}_{0.9})_2\text{Ca}_2\text{Cu}_3\text{O}_x$ (●) and for $(\text{Tl}_{0.8}\text{Bi}_{0.3})(\text{Ba}_{0.1}\text{Sr}_{0.9})_2\text{Ca}_2\text{Cu}_3\text{O}_y$ (○).

From this it follows that the $(1-F)$ value is constant for a field not exceeding the full penetration field H_{pf} . For the fields above H_{pf} $(1-F)$ depends on $1/H$. Using this dependency the field $H_{pf} = 1100$ A/m was estimated for (Tl,Pb)-sample. The screening properties of the (Tl,Bi)-sample are poor and the existence of the plateau is not very evident. Nevertheless, the penetration field $H_{pf} = 640$ A/m could be estimated for (Tl,Bi)-sample.

4. Conclusions

Pb doping of Tl-1223 samples resulted in better superconducting properties than Bi doping. (Tl,Pb)-samples show much more stronger inter-grain contacts. Their penetration magnetic fields are almost twice as great as for the (Tl,Bi)-samples. For (Tl,Pb)- and (Tl,Bi)-samples the first penetration magnetic fields (estimated by classical magnetization method) had values $H_{p1}^{wl} \sim 13.3$ A m⁻¹ and 8.6 A m⁻¹. Full penetration magnetic fields estimated by scanning Hall sensor method had values for $H_{pf} \sim 1100$ A/m and 640 A/m, respectively. In cases where the magnetic field penetration is determined mainly by geometrical barrier effects, H_{p1}^{wl} and H_{pf} could be the same, and then the agreement between the values of penetration fields obtained by magnetization and scanning Hall methods is notable.

Acknowledgements

This work was supported by the Slovak Grant Agency for Science (Projects No. 2/5086/98 and 2/1134/21) and by the Fonds zur Förderung der wissenschaftlichen Forschung in Österreich (Project: 13 945).

References

1. M. Mair, W. T. König and G. Gritzner, Supercond. Sci. Technol., **8** (1995) 894
2. V. Zrubec, A. Cigáň, J. Maňka, Physica C, **223** (1994) 90.
3. J. A. Osborn, Phys. Rev., **67** (1945) 351.
4. S. Reich, V. M. Nabutovsky, J. Appl. Phys., **68**, 668, (1990)